

Rare $B_{(s)}^0$ dileptonic decays at LHCb

A. MORDÁ on behalf of the LHCb COLLABORATION

CPPM, Aix-Marseille Université, CNRS/IN2P3 - Marseille, France

Aix-Marseille Université, CNRS, CPT, UMR 7332 - 13288 Marseille, France

Université de Toulon, CNRS, CPT, UMR 7332 - 83957 La Garde, France

ricevuto il 31 Luglio 2014

Summary. — Rare decays of B mesons are excellent tools to observe indirect hints of physics beyond the Standard Model. A summary of the searches for the rare dileptonic decays $B_{(s)}^0 \rightarrow \mu^+ \mu^-$ and $B_{(s)}^0 \rightarrow e^\pm \mu^\mp$ with the LHCb detector is presented in this contribution.

PACS 13.20.He – Decays of bottom mesons.

PACS 12.15.Mm – Neutral currents.

PACS 11.30.Hv – Flavor symmetries.

1. – Introduction

The lack of discovery in searches aiming to observe directly New Physics (NP) particles pushes their mass scale towards high values not reachable with direct searches. In this context, a complementary approach is given by indirect searches in the Heavy Flavor sector. The LHCb detector is designed to study B meson decays thanks to the high $b\bar{b}$ pair acceptance in pp collision, trigger efficiency, very good Particle IDentification and momentum resolution. In this contribution a summary of the searches for the rare dileptonic decays $B_{(s)}^0 \rightarrow \mu^+ \mu^-$ and $B_{(s)}^0 \rightarrow e^\pm \mu^\mp$ is presented.

2. – The $B_{(s)}^0 \rightarrow \mu^+ \mu^-$ channel

$B_{(s)}^0 \rightarrow \mu^+ \mu^-$ decays imply a Flavor Changing Neutral Current and are allowed in the Standard Model (SM) only at the loop level. For this reason, and also due to an additional helicity suppression, their rate is predicted to be very low and is very sensible to NP effects. The study of $B_{(s)}^0 \rightarrow \mu^+ \mu^-$ channels is then relevant to set constraints in the parameter space of several NP models.

The SM predictions for the branching fraction (BR) are [1]

$$\begin{aligned} (1) \quad & \text{BR}(B_s^0 \rightarrow \mu^+ \mu^-) = (3.65 \pm 0.23) \times 10^{-9}, \\ (2) \quad & \text{BR}(B^0 \rightarrow \mu^+ \mu^-) = (1.06 \pm 0.09) \times 10^{-10}. \end{aligned}$$

The first evidence for the $B_s^0 \rightarrow \mu^+ \mu^-$ mode has been obtained by the LHCb collaboration [2] with a significance of 3.5σ analyzing a 2.1 fb^{-1} dataset collected in 2011 (1 fb^{-1}) and 2012 (1.1 fb^{-1}) at $\sqrt{s} = 7$ and 8 TeV , respectively.

The analysis presented in this contribution has been updated in [3], by adding the remaining 1 fb^{-1} collected in the second half of 2012. In it, the number of observed $B_q^0 \rightarrow \mu^+ \mu^-$ ($q = s, d$) signal events in the dataset is converted into a value for the BR using the formula

$$(3) \quad \text{BR}(B_q^0 \rightarrow \mu^+ \mu^-) = \frac{\text{BR}_{\text{norm}}}{N_{\text{norm}}} \cdot \frac{\epsilon_{\text{norm}}}{\epsilon_{\text{sig}}} \cdot \frac{f_{\text{norm}}}{f_q} \times N_{B_q^0 \rightarrow \mu^+ \mu^-},$$

where BR_{norm} and N_{norm} the number and the BR of normalization channels respectively. The efficiencies $\epsilon_{\text{sig(norm)}}$ are the product of the trigger, reconstruction and selection efficiencies for signal and background. The factor f_{norm}/f_q is the ratio of probabilities that a b -quark hadronizes into a B_{norm} and a B_{sig} meson (f_u and f_d are assumed be equal). Normalization channels are chosen in order to have similar trigger efficiency ($B^+ \rightarrow J/\psi(\rightarrow \mu\mu)K^+$) or topology ($B^0 \rightarrow hh^{(\prime)}$ with $h^{(\prime)} = \pi, K$) of the $B_{(s)}^0 \rightarrow \mu^+ \mu^-$ signal. This allows to cancel possible systematics in the ratio $\epsilon_{\text{norm}}/\epsilon_{\text{sig}}$. For the analysis presented in this contribution the measured value of f_s/f_d obtained by LHCb using the dataset recorded at $\sqrt{s} = 7 \text{ TeV}$ [4] is used. $B_{(s)}^0 \rightarrow \mu^+ \mu^-$ candidates are selected requiring two opposite charged tracks forming a displaced vertex with respect to any other primary vertex, a transverse momentum in the range $[0.25, 40] \text{ GeV}$ and a momentum smaller than 500 GeV .

The most important source of background in the signal mass search window (defined in the range $[M_{B_d^0} - 60 \text{ MeV}/c^2, M_{B_d^0} + 60 \text{ MeV}/c^2]$) comes from combinatorial $b\bar{b} \rightarrow \mu^+ \mu^- X$ events originating by random combinations of muons coming from semi-leptonic B decays. The B^0 mass search window is also polluted from the physical mode $B_{(s)}^0 \rightarrow hh^{(\prime)}$ where both hadrons are misidentified as muons. Other exclusive modes, with misidentified hadrons ($B^0 \rightarrow \pi^- \mu^+ \nu_\mu$, $B_s^0 \rightarrow K^- \mu^+ \nu_\mu$, $\Lambda_b \rightarrow p \mu \nu_\mu$, $B_{(s)}^0 \rightarrow hh^{(\prime)}$) or two muons coming from a same displaced vertex ($B^{0/+} \rightarrow \pi^{0/+} \mu\mu$, $B_c \rightarrow J/\Psi(\mu\mu)\mu\nu_\mu$), peak at lower values of the di-muon invariant mass $m_{\mu\mu}$.

Events are classified in a two dimensional plane according to $m_{\mu\mu}$ and the output of a Boosted Decision Tree (BDT). To avoid unconscious biases, candidate events in the signal mass regions are not examined up to the analysis completion. The BDT classifier is trained on Monte Carlo generated samples for combinatorial background and signal events, using 12 kinematical and topological variables. The output of this classifier is by design flat between 0 and 1 for signal Monte Carlo and peaks at 0 for combinatorial background events, as shown in fig. 1.

The BDT shape for signal events is calibrated on data using a sample of exclusive $B_{(s)}^0 \rightarrow hh^{(\prime)}$. For background events the BDT shape is obtained interpolating the mass sidebands into the signal region with an exponential function. The invariant mass shape for signal is described by a Crystal Ball function with its mean calibrated using exclusive $B_{(s)}^0 \rightarrow hh^{(\prime)}$ decays and its resolution evaluated using the di-muon resonances

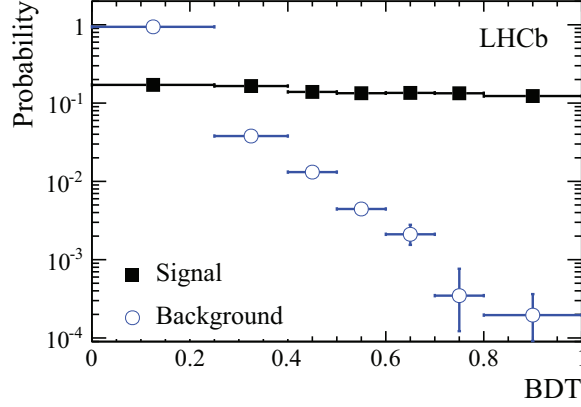


Fig. 1. – Expected distribution of the BDT output for the $B_s^0 \rightarrow \mu^+ \mu^-$ signal (black squares), obtained from $B_{(s)}^0 \rightarrow hh^{(\prime)}$ control channels, and the combinatorial background (blue circles).

and $B_{(s)}^0 \rightarrow hh^{(\prime)}$ decays. The combinatorial mass shape is obtained by fitting the data sidebands with an exponential function. The peaking background is assumed to have the same BDT distribution as the signal, while its mass shape is evaluated from simulated events.

The event yields are determined through a simultaneous unbinned likelihood fit performed in a projection of $m_{\mu\mu}$ in 8 BDT bins. The yields of $B_s^0 \rightarrow \mu^+ \mu^-$, $B^0 \rightarrow \mu^+ \mu^-$ and the combinatorial background are left free, while the yields and shapes of the exclusive modes are constrained. An excess of events at the B_s^0 mass value is observed with a signal strength of 4σ , together with a lower excess (only 2σ) at the B^0 mass, corresponding to the following values for the BR:

$$(4) \quad \text{BR}(B_s^0 \rightarrow \mu^+ \mu^-) = 2.9_{-1.0}^{+1.1} \times 10^{-9},$$

$$(5) \quad \text{BR}(B^0 \rightarrow \mu^+ \mu^-) = 3.7_{-2.1}^{+2.4} \times 10^{-10}.$$

The fit results for events with a value of BDT greater than 0.7 is shown in fig. 2.

Since no significant excess is observed for the $B^0 \rightarrow \mu^+ \mu^-$ decay, an upper limit is set using the CL_s approach. The distribution of the CL_s as a function of the various hypothesis on the $\text{BR}(B^0 \rightarrow \mu^+ \mu^-)$ is shown in fig. 3. The obtained upper limit is

$$(6) \quad \text{BR}(B^0 \rightarrow \mu^+ \mu^-) < 6.3 (7.4) \times 10^{-10} \text{ @ } 90 (95)\% \text{ C.L.}$$

The obtained values (4)-(6) are consistent with the SM predictions and, even if they still leave some room, they rule out huge NP effects.

3. – $B_{(s)}^0 \rightarrow e^\pm \mu^\mp$

The Lepton Flavor Violating mode $B_{(s)}^0 \rightarrow e^\pm \mu^\mp$ is forbidden in the SM and has never been observed. In some NP scenarios it could take place thanks to the mediation of Lepto-Quark (LQ) particles.

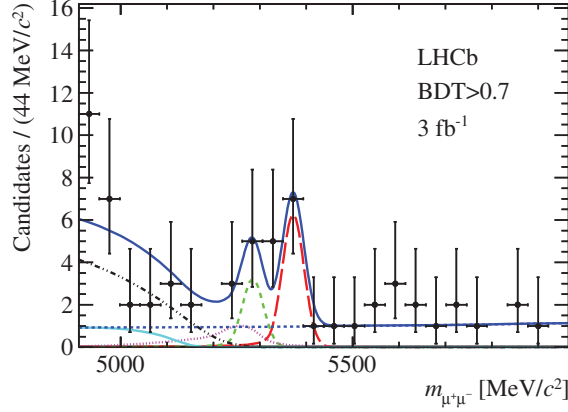


Fig. 2. – Invariant-mass distribution of the selected $B_{(s)}^0 \rightarrow \mu^+\mu^-$ candidates (black dots) with $\text{BDT} > 0.7$. The result of the fit is overlaid (blue solid line) and the different components detailed: $B_s^0 \rightarrow \mu^+\mu^-$ (red long-dashed line), $B^0 \rightarrow \mu^+\mu^-$ (green medium-dashed line), combinatorial background (blue medium-dashed line), $B_{(s)}^0 \rightarrow hh^{(\prime)}$ (magenta dotted line), $B^{0(+)} \rightarrow \pi^{0(+)}\mu^+\mu^-$ (light blue dot-dashed line), $B^0 \rightarrow \pi^-\mu^+\nu_\mu$ and $B^0 \rightarrow K^-\mu^+\nu_\mu$ (black dot-dashed line).

The previous best upper limits on the BR of these decays were obtained by the CDF collaboration [5]:

$$(7) \quad \text{BR}(B^0 \rightarrow e^\pm\mu^\mp) < 64.0 (79.0) \times 10^{-9} \text{ @ } 90 (95)\% \text{ C.L.},$$

$$(8) \quad \text{BR}(B_s^0 \rightarrow e^\pm\mu^\mp) < 20.0 (20.6) \times 10^{-8} \text{ @ } 90 (95)\% \text{ C.L.}$$

The LHCb analysis presented in this contribution is based on 1 fb^{-1} collected by

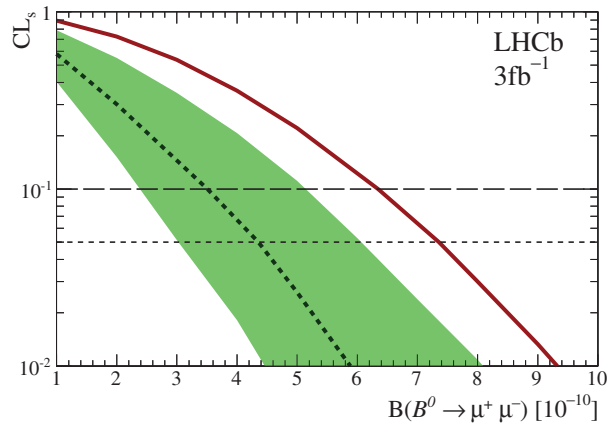


Fig. 3. – CL_s as a function of the assumed $B^0 \rightarrow \mu^+\mu^-$ branching fraction. The dashed curve is the median of the expected CL_s distribution for the background-only hypothesis. The green area covers the 1σ region. The solid red curve is the observed CL_s .

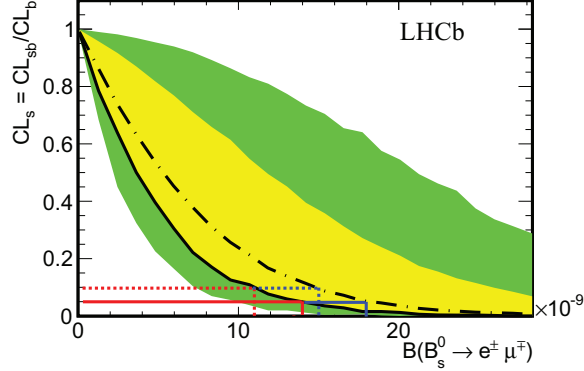


Fig. 4. – CL_s as a function of the branching fraction for $B_s^0 \rightarrow e^\pm \mu^\mp$ decay. The dashed lines are the expected CL_s in the background-only hypothesis. The yellow (green) area represents the 1σ (2σ) region of the expected CL_s distribution. The solid lines represent the observed CL_s . The upper limits at 90% and 95% are indicated by a dotted and a solid blue lines, respectively, for the expectation and by red lines for the observation.

LHCb in 2011 at $\sqrt{s} = 7\text{ TeV}$ and inherits most of the features of the $B_{(s)}^0 \rightarrow \mu^+ \mu^-$ analysis [6]. To avoid biases, events in the signal regions are not examined up to the completion of the analysis.

The dominant source of background is represented by random combinations of e and μ coming from two different B semileptonic decays. As in the $B_{(s)}^0 \rightarrow \mu^+ \mu^-$, the discrimination of the $B_{(s)}^0 \rightarrow e^\pm \mu^\mp$ signal against this background is achieved exploiting the topological and kinematical information of each candidate. Other exclusive modes could fake the $B_{(s)}^0 \rightarrow e^\pm \mu^\mp$ signal, in particular $\Lambda_b \rightarrow p\mu\nu_\mu$, $B_{(s)}^0 \rightarrow hh^{(\prime)}$, $B_c \rightarrow J/\Psi(\mu\mu)e\nu_e$, $B_c \rightarrow J/\Psi(ee)\mu\nu_\mu$, and the peaking background $B_{(s)}^0 \rightarrow hh^{(\prime)} \rightarrow e\mu$.

Events are classified in a two dimensional plane according to their electron-muon invariant mass $m_{e\mu}$ and the output of a BDT trained on Monte Carlo generated samples (both for signal and background) using geometrical and kinematic variables.

The invariant mass shape of the $B_{(s)}^0 \rightarrow e^\pm \mu^\mp$ signal is a Crystal Ball function the parameters of which are obtained from simulation, while the BDT shape is calibrated using the $B_{(s)}^0 \rightarrow hh^{(\prime)}$ control channel. The invariant mass and BDT shape for combinatorial background inside the signal window search are obtained by interpolating the invariant mass sidebands in bins of BDT.

The number of expected events is converted into a value for the BR using the relation (3) where the normalization channel is chosen to be $B^0 \rightarrow K^+ \pi^-$.

The observed distribution of events in the invariant mass - BDT output is compared with the expected distribution for a given hypothesis on the BR using the CL_s method. Figure 4 shows the expected and observed CL_s as a function of the BR($B_{(s)}^0 \rightarrow e^\pm \mu^\mp$).

No significant signal is observed, and the following upper limits the BR are found:

$$(9) \quad \text{BR}(B_s^0 \rightarrow e^\pm \mu^\mp) < 1.1 (1.4) \times 10^{-8} \text{ @ } 90 (95)\% \text{ C.L.},$$

$$(10) \quad \text{BR}(B^0 \rightarrow e^\pm \mu^\mp) < 2.8 (3.7) \times 10^{-9} \text{ @ } 90 (95)\% \text{ C.L.},$$

which are a factor ~ 20 more stringent than (7) and (8).

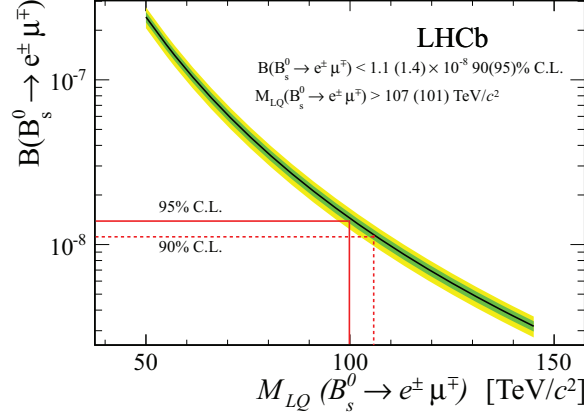


Fig. 5. – Branching fraction as a function of the mass of the lepto-quark for the $B_s^0 \rightarrow e^\pm \mu^\mp$. The green (yellow) area represents the 1σ (2σ) region.

One of the NP models which deals with lepto-quark is the Pati-Salam model [7] in which the requirement of local symmetry between quarks and leptons leads to the existence of a set of spin-1 lepto-quark carrying color and lepton quantum number. In this model the BR of the $B_{(s)}^0 \rightarrow e\mu$ is related to the mass of the lepto-quark (as shown in fig. 5 for the case of the $B_s^0 \rightarrow e\mu$ decay). The upper limits (9) and (10) imply the following lower bounds on the mass of the lepto-quark mediating the decays:

$$(11) \quad m_{LQ_s}(B_s^0 \rightarrow e^\pm \mu^\mp) > 107 (101) \text{ TeV}/c^2 @ 90 (95)\% \text{ C.L.},$$

$$(12) \quad m_{LQ_d}(B^0 \rightarrow e^\pm \mu^\mp) > 135 (126) \text{ TeV}/c^2 @ 90 (95)\% \text{ C.L.}$$

4. – Conclusions

Rare B meson decays are a powerful tool to look for indirect hints of NP beyond the SM. The LHCb collaboration has measured several of these processes with a unique precision.

In this contribution the update of the $B_{(s)}^0 \rightarrow \mu^+\mu^-$ analysis based on 3.1 fb^{-1} collected in 2011 and 2012 has been presented. The analysis confirms the evidence for $B_{(s)}^0 \rightarrow \mu^+\mu^-$ with a significance 4.0σ and a $\text{BR}(B_{(s)}^0 \rightarrow \mu^+\mu^-) = 2.9_{-1.0}^{+1.1} \times 10^{-9}$ and puts a lower upper limit on the BR of $B^0 \rightarrow \mu^+\mu^-$.

The search for the LFV modes $B_{(s)}^0 \rightarrow e^\pm \mu^\mp$ at LHCb has also been presented. The first LHCb results, based on 1 fb^{-1} of data collected at $\sqrt{s} = 7 \text{ TeV}$, improve previous measurements by a factor ~ 20 .

* * *

This work has been carried out thanks to the support of the OCEVU Labex (ANR-11-LABX-0060) and the A*MIDEX project (ANR-11-IDEX-0001-02) funded by the “Investissements d’Avenir” French government program managed by the ANR.

REFERENCES

- [1] BOBETH C. *et al.*, ArXiv:1311.0903v1.
- [2] AAIJ R. *et al.* (LHCb COLLABORATION), *Phys. Rev. Lett.*, **110** (2013) 021801.
- [3] AAIJ R. *et al.* (LHCb COLLABORATION), *Phys. Rev. Lett.*, **111** (2013) 101805.
- [4] AAIJ R. *et al.* (LHCb COLLABORATION), LHCb-CONF-2013-011, (2013).
- [5] AALTONEN T. *et al.* (CDF COLLABORATION), *Phys. Rev. Lett.*, **102** (2009) 201901.
- [6] AAIJ R. *et al.* (LHCb COLLABORATION), *Phys. Rev. Lett.*, **111** (2013) 141801.
- [7] PATI J. C. and SALAM A., *Phys. Rev. D*, **10** (1974) 275.